Key Engineering Materials
ISSN: 1662-9795, Vol. 926, pp 784-801
doi:10.4028/p-s91nhk

Submitted: 2021-12-08
Revised: 2022-02-04
Accepted: 2022-02-08
Online: 2022-07-22

Effects of Temperature on Deep Drawing of an Aluminum Alloy for Different Yield Criteria and Hardening Models

Rasih Hakan Demirkol[1,a*], Haluk Darendeliler[1,b]

[1]Department of Mechanical Engineering, Middle East Technical University, Ankara 06800, Turkey

[a]rhdemirkol@aselsan.com.tr, [b]hdarende@metu.edu.tr

Keywords: Deep Drawing, Yield Criteria, Hardening Models.

Abstract. In this study, the influences of temperature variation in deep drawing process are investigated by changing the temperatures of the whole blank, a part of the blank, the punch and die for different yield criteria and hardening models. Von-Mises criterion with isotropic, kinematic and combined hardening and, Hill48 and Yld2003 yield criteria with isotropic hardening are considered to form the constitutive relations. Circular, square and complex shaped parts made of AA5754 material are used in the numerical analyses. The local heating simulations are conducted for circular blanks and the drawability of the parts are evaluated by using the Johnson-Cook failure criteria. Hot forming and quenching and local heating analyses are also carried out for a complex shaped part. The results obtained by the finite element analyses for different constitutive equations are compared with each other and experimental results according to thickness strain distribution, punch force variation and rim shape of the deformed blanks.

Introduction

The temperatures of the sheet metal, the punch and the die are important parameters for sheet metal forming processes since temperature affects directly ductility of the material as well molecular-atomic structure, and in some cases, room temperature may not be enough to obtain properly drawn blank without defects. To determine the appropriate parameters and effects of the heating methods and temperature on formability, experimental methods are generally used in deep drawing process. Basril et al. [1] experimentally investigated effects of temperature and heating methods on formability of square cup deep drawing process by heating die only, punch only and heating both. By comparing thickness distribution of aluminum, mild steel and stainless steel materials for four different temperatures, optimal result was obtained to get uniform thickness distribution.

Although the experimental method is reliable, but not time and cost effective, numerical methods such as finite element analysis are preferred to design the forming processes. In recent decades, a number of new anisotropic yield criteria were introduced to analyze sheet forming processes at different temperatures. Laurent et al. studied on effects of temperature and friction coefficients on deep drawing process of an AA5754-O alloy sheet [2]. A coupled thermo-mechanical FE model and different yield criteria such as von Mises and Hill48 were used. The blank was formed by heating die and blank holder. They also compared the numerical and experimental results. Abedrabbo et al. [3] developed a temperature dependent, anisotropic yield criterion to show formability of two different aluminum alloys (5182 and 5754) used in automobile industry by a coupled thermo mechanical finite element analysis. The anisotropy coefficients of the YLD2000-2d model [4] were determined for different temperatures from 25°C to 260°C experimentally. Authors determined the failure by using strain and stress-based forming limit diagrams.

In the solution heat treatment, forming, and in-die quenching (HFQ) process [5], the sheet is heated up to solution heat treatment (SHT) temperature, and consequently the alloying elements or precipitates dissolve within the aluminum material. As a result, the used material becomes more ductile with a lower yield stress and any complex shape can be easily formed at a higher speeds. After then, the in-die quenching process takes place and the formed part, as a supersaturated solid solution, has an increased strength. Fakir et al. studied HFQ process for AA5754-O material numerically [6]. Good correlation

was obtained between simulated and experimentally formed shapes with respect to thickness distribution. Moreover, effects of forming temperature and forming speed on the thickness distribution of the HFQ parts were investigated. It was observed that higher forming speed is more beneficial for HFQ forming since it led to less thinning and more uniform shape. For FE model of HFQ process, to include deformation and heat transfer mechanisms, 8-node thermally coupled brick elements were used.

In this study, the effects of temperature variation on thickness strain distribution, punch force variation and rim shape of the deformed blanks in deep drawing process are investigated. Different heating approaches are used such as uniform heating of the blank, punch and die, local heating of blank and applying HFQ process. The constitutive models are formed through the use of von-Mises criterion with isotropic, kinematic and combined hardening and, Hill48 and Yld2003 yield criteria with isotropic hardening. Circular, square and complex shaped parts made of AA5754 material are used in the numerical analyses. The results obtained by the finite element analyses for different constitutive equations are compared with each other and experimental results. By using the Johnson-Cook failure criteria, drawability of the locally heated circular blanks are evaluated.

Constitutive Models

Von Mises Yield Criterion. Von-Mises yield criterion [7] is one of the mostly known and used yield criteria in plasticity problems. This criteria can be expressed for isotropic hardening rule as:

$$\sigma'_{ij}\sigma'_{ij} = \frac{2}{3}\sigma_Y^2 \tag{1}$$

where σ'_{ij} and σ_Y represent the deviatrotic stress components and the yield stress, respectively.

Von Mises yield criteria with kinematic hardening rule [7] is described as,

$$(\sigma'_{ij} - \alpha_{ij})(\sigma'_{ij} - \alpha_{ij}) = \frac{2}{3}\sigma_{Y^0}^2 \tag{2}$$

where σ_{Y^0} is the initial yield stress of the used material and α_{ij} is the backstress tensor.

The yield criteria with combined hardening rule [7], which is combination of isotropic and kinematic hardening rules, can be expressed as,

$$(\sigma'_{ij} - \alpha_{ij})(\sigma'_{ij} - \alpha_{ij}) = \frac{2}{3}\sigma_Y^2 \tag{3}$$

Hill48 Yield Criteria. This criteria is an anisotropic yield criteria which is proposed by Hill [8] and has quadratic function as given below,

$$\begin{aligned} 2f(\sigma_{ij}) = {} & F(\sigma_{33} - \sigma_{22})^2 + G(\sigma_{11} - \sigma_{33})^2 + H(\sigma_{22} - \sigma_{11})^2 \\ & + 2L(\sigma_{23})^2 + 2M(\sigma_{31})^2 + 2N(\sigma_{12})^2 - 1 \end{aligned} \tag{4}$$

where F, G, H, L, M and N are the material constants for anisotropy.

Johnson Cook Model. This plasticity model [9] describes the flow stress depending on strain, strain rate and temperature as given below:

$$\sigma = (A + B\varepsilon^n)(1 + Cln(\frac{\dot{\varepsilon}}{\dot{\varepsilon}_{ref}}))(1 - (\frac{T - T_{ref}}{T_m - T_{ref}})^m) \tag{5}$$

In this model, A, B and n are the strain hardening constants, C is the material constant which is related to the strain rate characteristic, and m is a constant for temperature-dependent part of model. ε, $\dot{\varepsilon}$, $\dot{\varepsilon}_{ref}$, T, T_m and T_{ref} correspond strain and temperature dependent parameters.

YLD2003-8P Yield Criteria. This yield criterion [10] has eight anisotropy parameters which are a_1,. . .,a_8 and given as;

$$|\sigma_1{}'|^m + |\sigma_2{}'|^m + |\sigma_1{}'' - \sigma_2{}''|^m = 2Y_{ref}^m \tag{6}$$

$$\sigma_1{}' = \frac{a_8\sigma_{11} + a_1\sigma_{22}}{2} + \sqrt{(\frac{a_2\sigma_{11} - a_3\sigma_{22}}{2})^2 + a_4\sigma_{21}\sigma_{12}} \tag{7}$$

$$\sigma_2{}' = \frac{a_8\sigma_{11} + a_1\sigma_{22}}{2} - \sqrt{(\frac{a_2\sigma_{11} - a_3\sigma_{22}}{2})^2 + a_4\sigma_{21}\sigma_{12}} \tag{8}$$

$$\sigma_1{}'' = \frac{\sigma_{11} + \sigma_{22}}{2} + \sqrt{(\frac{a_5\sigma_{11} - a_6\sigma_{22}}{2})^2 + a_7\sigma_{21}\sigma_{12}} \tag{9}$$

$$\sigma_2{}'' = \frac{\sigma_{11} + \sigma_{22}}{2} - \sqrt{(\frac{a_5\sigma_{11} - a_6\sigma_{22}}{2})^2 + a_7\sigma_{21}\sigma_{12}} \tag{10}$$

The anisotropy parameters a_1,. . .,a_8 that are given in Eq.(6) can be used to fit the yield criterion to selected experimental data obtained from mechanical test or calculated from polycrystalline models [7]. Y_{ref} is a reference yield stress of the considered material and m is a material constant depends on the material crystal structure. While m is 6 for BCC crystal structure, it is 8 for FCC crystal structure. The yield function corresponding to Eq. (6) is given by:

$$f(a_i, \sigma) = \bar{\sigma}(a_i, \sigma) - Y_{ref} \leq 0 \tag{11}$$

with the equivalent stress:

$$\bar{\sigma}(a_i, \sigma) = (\frac{|\sigma_1{}'|^m + |\sigma_2{}'|^m + |\sigma_1{}'' - \sigma_2{}''|^m}{2})^{1/m} \tag{12}$$

The following error function in Eq. (13) is to be minimized to calculate the anisotropy parameters.

$$(\frac{\bar{\sigma_b} - Y_{ref}}{Y_{ref}})^2 + \sum_{i=1}^{3}(\frac{\bar{\sigma_{\phi_i}} - Y_{ref}}{Y_{ref}})^2 + (\frac{r_b - r_b^{exp}}{r_b^{exp}})^2 + \sum_{i=1}^{3}(\frac{r_{\phi_i} - r_{\phi_i}^{exp}}{r_{\phi_i}^{exp}}) = min \tag{13}$$

where σ_b is the equibiaxial yield stress and corresponding value of r_b can be obtained from a cross tensile test or a bulge test.

Finite Element Analysis

In this study, deep drawing processes of cylindrical, square and irregular complex shaped blanks were simulated for different temperatures by using the finite element analysis package ABAQUS. Moreover, analyses of locally heated circular and complex shaped blanks that were carried out. Only a quarter of the blanks were modeled in simulations of cylindrical and square blanks. Von Mises yield criterion, Hill48 yield criterion and Johnson Cook model were directly used from ABAQUS library. The other yield criterion, YLD2003-8p, was implemented through the VUMAT subroutine.

In cylindrical and square cup drawing, the blanks were defined as deformable bodies, however the die, the blank holder and the punch were modeled as rigid bodies. Four node shell elements with reduced integration (S4R4) were selected to form the mesh for the simulations where thermal effects were not considered.

For the thermo-mechanical analysis of cylindrical cup drawing, in which, initial temperatures of punch, die and blank were separately defined and C3D8RT elements were used to form the mesh. Moreover, the heat conduction between the surfaces was defined by applying contact condition between the blank and tools.

In the analysis of complex shaped part, by defining initial temperature values to the different regions of the blank, a thermo-mechanical analysis was carried out. While C3D4T elements were used to form the mesh in the local heating stage of the blank, explicit, 8-node thermally coupled brick elements (C3D8T) were used. To simulate the deformation of blank and heat transfer between the blank and the tools. All tools were modelled as deformable bodies.

Results and Discussion

The results obtained for different constitutive equations by the finite element analyses are compared with each other and experimental results according to thickness strain distribution, punch force and rim shape.

Deep Drawing of Cylindrical Blanks. Mechanical properties and density, Johnson Cook and Lankford parameters for AA5754-O material are presented in Tables 1, 2 and 3, respectively. True stress-strain curves for AA5754 material at room temperature, 175°C and 250°C that were obtained from study of Winklhofer et al. are shown in Figure 1. The dimensions of all tools of cylindrical cup deep drawing are presented in Table 4.

Table 1: Mechanical properties and density of AA5754 [11]

Young Modulus E (GPa)	71
Poisson's Ratio	0.33
Density (kg/m^3)	2700

Table 2: Johnson Cook Parameters of AA5754 [12]

A (MPa)	B (MPa)	C	n	m	$\dot{\varepsilon}$ (s^{-1})
28.13	278.67	0.00439	0.183	2.527	0.1

Table 3: Lankford Parameters of AA5754 [13]

Θ	r_Θ
0°	0.85
45°	0.67
90°	0.7

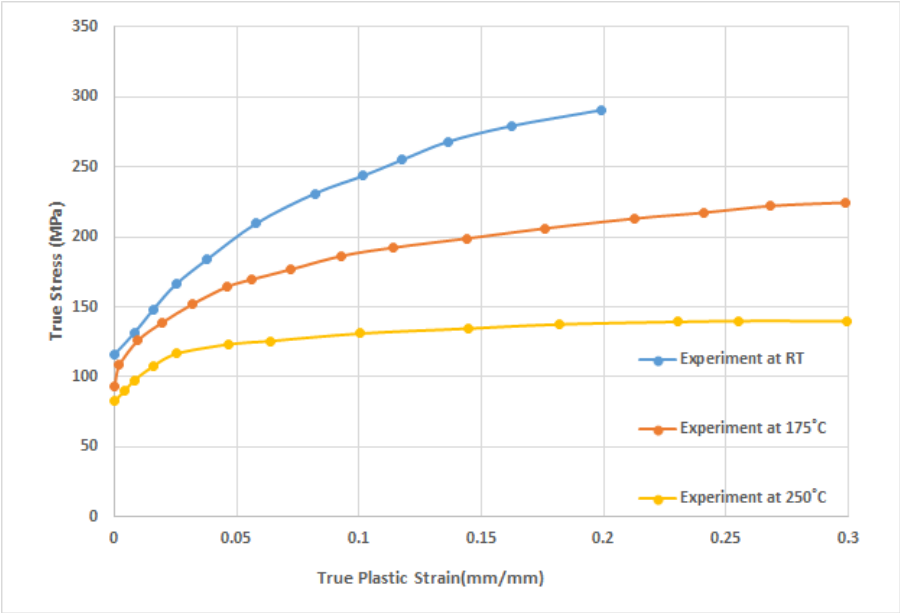

Fig. 1: True stress-strain curve of AA5754-O at room temperature, 175°C and 250°C [11].

Table 4: Dimensions of the tools of the cylindrical cup deep drawing [11]

Diameter of Blank (mm)	230
Diameter of Punch (mm)	110
Diameter of Punch Shoulder (mm)	10
Diameter of Die (mm)	113
Diameter of Die Shoulder (mm)	15

The experimental results for cylindrical deep drawing were taken from study of Winklhofer et al. [11]. Used yield criteria are compared with experimental results at room temperature, 175°C and 250°C for 80 mm punch travel.

Thickness strain distributions of the deep drawn cylindrical cup at room temperature are shown in Figure 2 for all yield criteria. Except Hill48 and von Mises yield criteria with kinematic hardening rule, other models gave close results to experimental ones for all parts of the blank. Results of the thickness strain distributions of the Hill48 and von Mises yield criteria with kinematic hardening rule approximates the experimental results only at the flange region. The closest result to the experimental result was obtained from YLD2003-8p yield criterion and results for von Mises yield criterion with kinematic hardening rule deviate significantly from experimental results.

Thickness strain distributions of deep drawn cylindrical cup at 175°C are shown in Figure 3 and they show almost same trend with results at room temperature. Results of thickness strain distribution for the Von-Mises yield criterion with kinematic hardening rule is significantly different from results of the experiment and other models at the region under the punch. At this region, the results of Hill48 yield criterion also deviated from the experimental results. YLD2003 yield criterion gave the best result for this case.

Thickness strain distributions of the deep drawn cylindrical cup at 250°C are shown in Figure 4 for all mentioned yield criteria. Except von Mises yield criterion with kinematic hardening rule, other yield criteria have closer results to experimental result for all parts of the blank. Result of the YLD2003-8p yield criterion is in better agreement with experimental result for all parts of the blank. While result of thickness strain distribution of the Von-Mises yield criterion with kinematic hardening rule is significantly different from results of the experiment and other models at the region under the

punch, this model gives a good result at the flange region. Hill48 yield criterion gives better result at 250°C than room temperature and 175°C for the region under the punch.

In Figures 5-7, variation of punch force with punch displacement are shown for room temperature, 175°C and 250°C, respectively. The maximum punch displacement was taken as 80 mm for all yield criteria. For all yield criteria, after 35 mm punch displacement, punch force values start to decrease except von Mises yield criteria with kinematic hardening rule. By comparing these three figures, it is observed that punch force value decreases with increasing temperature.

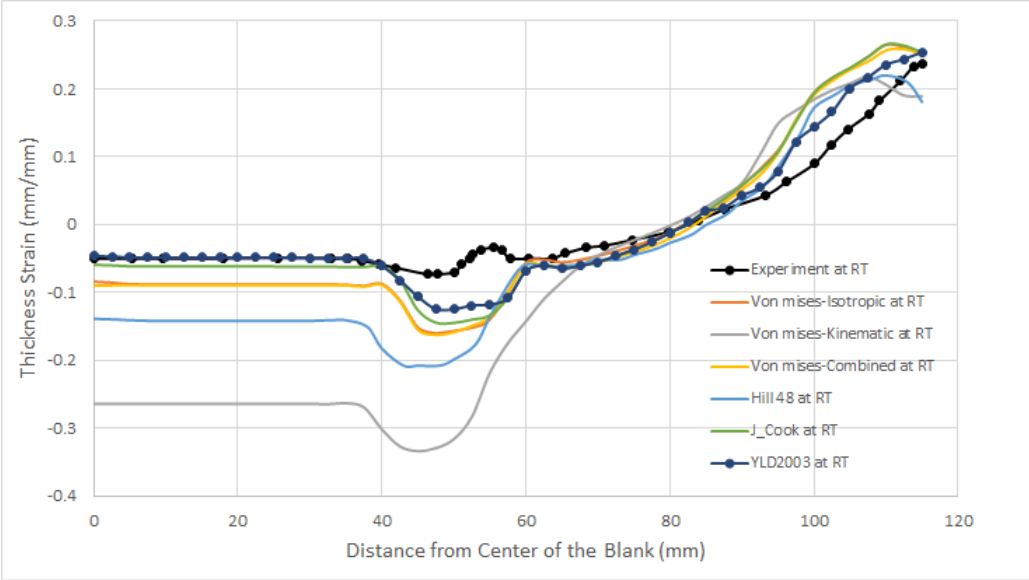

Fig. 2: Thickness strain distributions for different models and experiment at room temperature (Cylindrical, 80 mm punch travel)

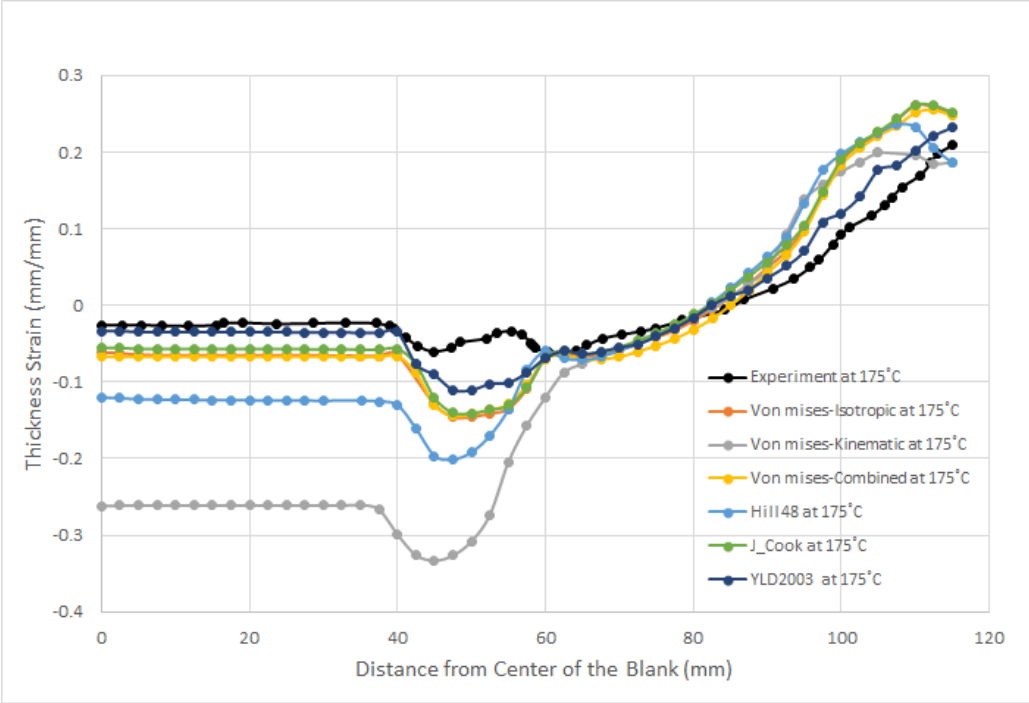

Fig. 3: Thickness strain distributions for different models and experiment at 175°C (Cylindrical, 80 mm punch travel)

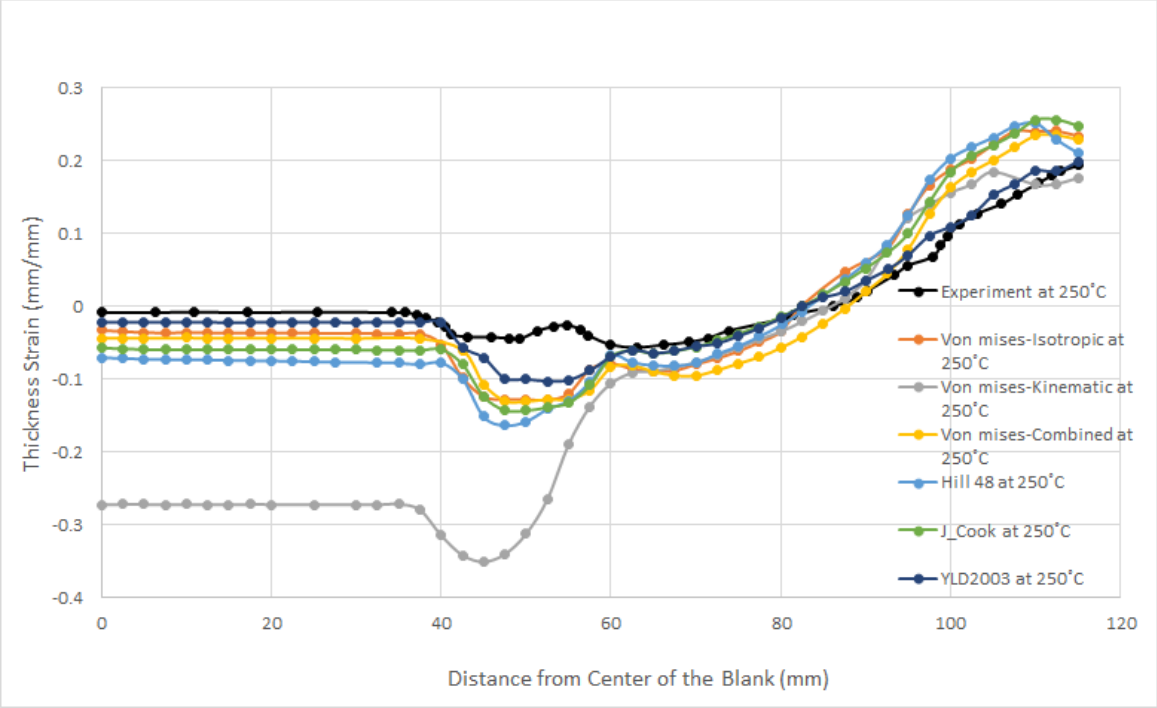

Fig. 4: Thickness strain distributions for different models and experiment at 250°C (Cylindrical, 80 mm punch travel)

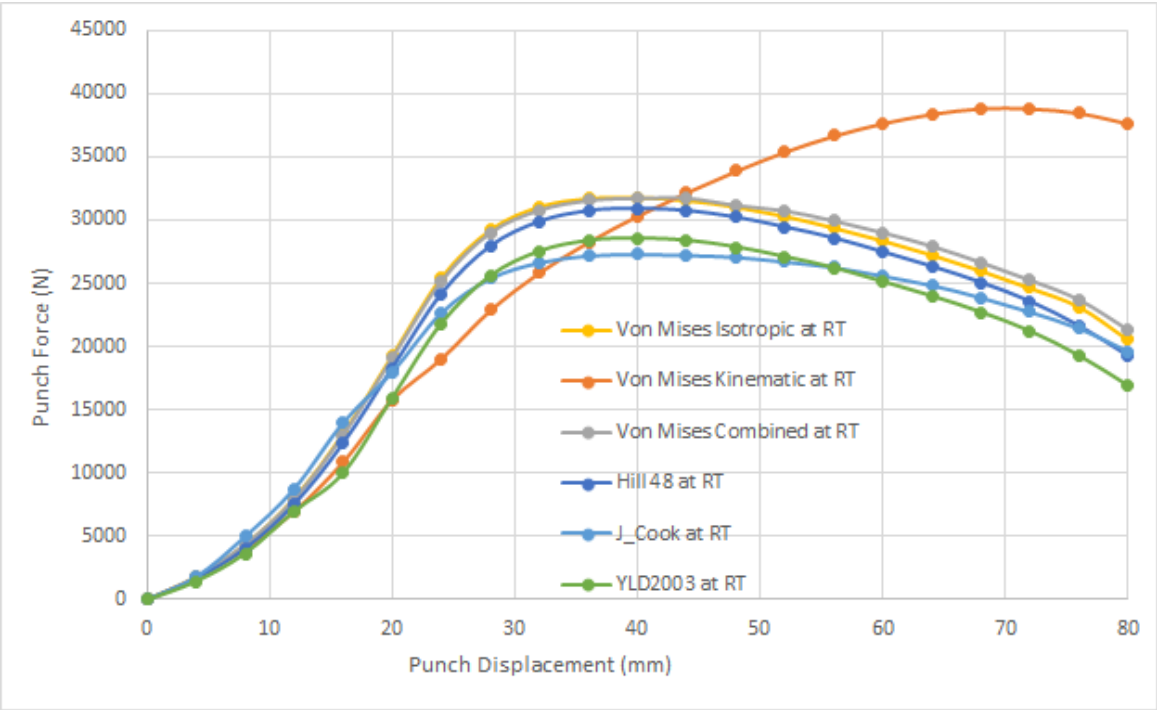

Fig. 5: Punch force vs cylindrical punch displacement at room temperature for different models

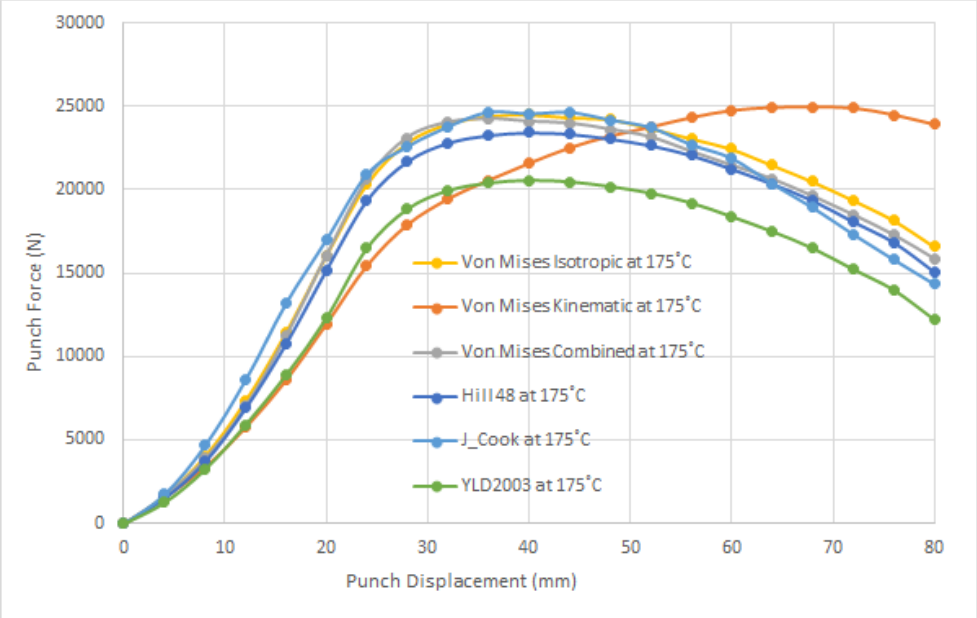

Fig. 6: Punch force vs cylindrical punch displacement at 175°C for different models

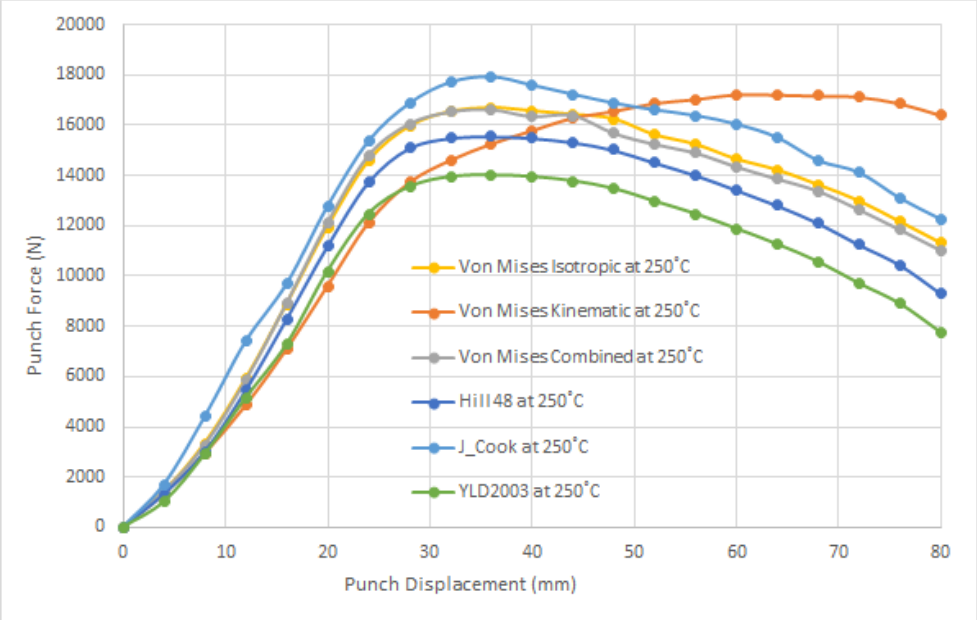

Fig. 7: Punch force vs cylindrical punch displacement at 250°C for different models

It can be obsereved from simulations that radius of the rim shape of the deformed blank becomes smaller with decreasing temperature. The predicted flow of the blank into the die cavity is larger for Hill48 and YLD2003 yield criteria. Variations of the radius value increased at the middle of the edge of the quarter rim shape.

Deep Drawing of Square Blanks. YLD2003-8p yield criterion was used to determine the thickness strain distribution and punch force variation are given for 25 mm punch travel at room temperature, 300°C and 520°C for a square blank. The dimensions of the tools and square blank are presented in Table 5. The same material which has been used cylindrical drawing was selected as blank material.

In Figure 8, effects of temperature variation on thickness strain distributions of deep drawn square cup are shown. Thickness strains and thinning of the sheet decreased with increasing temperature at the region under the punch, however; thickness strain and thickening increased at the flange region.

Table 5: Dimensions of the tools of the square cup deep drawing [7]

Blank Dimension (mm)	80 x 80
Punch Dimension (mm)	40 x 40
Punch Shoulder Diameter (mm)	12
Die Dimension (mm)	42 x 42
Die Shoulder Diameter (mm)	4.5

In Figure 9, variations of punch forces with punch displacements are shown at room temperature, 300°C and 520°C. Punch force decreases with increasing temperature. The diminish of increase of punch force after 15 mm punch travel indicates the occurrence of tensile instabilities.

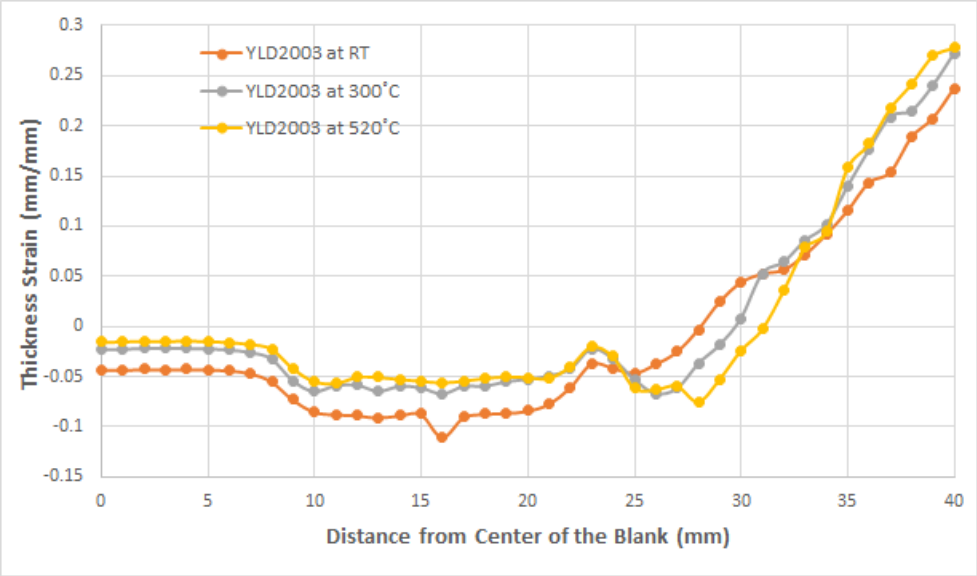

Fig. 8: Effect of temperature on thickness strain distributions for YLD2003 (Square, 25 mm punch travel)

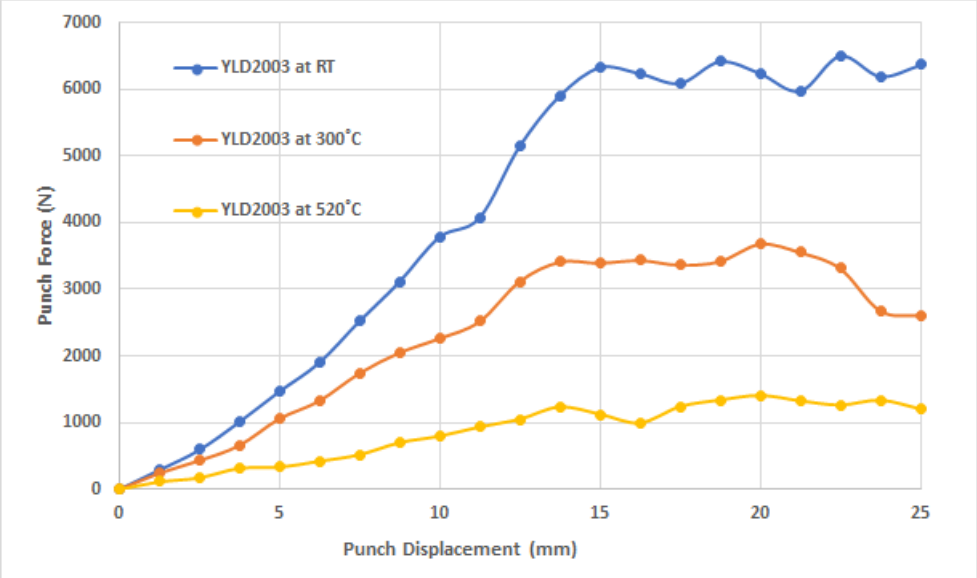

Fig. 9: Punch force vs square punch displacement at different temperatures for YLD2003-8P

It was observed that area of the rim shape of the deformed shape became larger with increasing temperature. There are not any deviations between rim shapes for room temperature, 300°C and 520°C at the corners of the rim shapes. Variations of the predicted flow of the blank into the die cavity were easily observed at other parts of the edges of the blanks.

Local Heating in Deep Drawing Circular Blanks. In the analyses of local heating in deep drawing of circular blanks, AA5754-O material was used for blank, and XC38CrMoV5 material was used for die and punch. The thermal and mechanical properties of both materials were taken from study of Laurent et al., and are presented in Table 6.

To observe the local heating effects on thickness strain distributions, four different cases were considered. The temperature values used for blank, die and punch in these cases are given in Table 7. The blank was divided into two parts as flange and inner part to define the different temperature values. The results were given up to for 80 mm punch travel. The dimensions of the used blank, punch and die are given in Table 4.

Table 6: Thermal and mechanical properties of blank and tool material [11] and [2]

	Blank Material	Tool Material
Property	AA5754-O	XC38CrMoV5
Density	2700 kg/m^3	8150 kg/m^3
Young's Modulus	71 GPa	215 GPa
Poisson's ratio	0.33	0.3
Thermal expansion coefficient	2.4*10^{-5} 1/K	1.9*10^{-5} 1/K 1/K
Heat capacity	920 J/kgK	500 J/kgK
Heat conduction	121 W/mK	25 W/mK

It was observed that at in Case 3, Johnson Cook failure criterion predicted the failure at 62.2 mm punch travel by a fracture that occurred near the punch corner. Therefore, any data related to Case 3 is not presented in Figure 10 and 11.

Table 7: Temperature of the tools and regions of the blank in local heating processes

	Case-1	Case-2	Case-3	Case-4
Initial Temp. of Inner Part of Blank (°C)	25	25	175	175
Initial Temp. of Flange (°C)	25	175	25	175
Temperature of Die (°C)	25	175	25	175
Temperature of Blank Holder (°C)	25	175	25	175
Temperature of Punch (°C)	25	25	175	175

Figure 10 shows the temperature distribution of the undeformed and formed blanks. In Case 1, although initial temperatures of the blank and all tools are 25°C, temperature increased with deformation especially at the highly deformed regions due to the plastic work. Similar trend can be also seen in other cases. Temperature values increase about 40°C at these regions.

Thickness strain distributions obtained for Cases 1, 2 and 4, experimental results observed at room temperature and 175°C are in Figure 11. For homogeneous temperature distribution (Case 1 and Case 4) thickness strain decreases with increasing temperature. When only the flange region of the blank is heated and the inner region of the blank is kept at room temperature as in Case 2, more uniform thickness strain distribution is obtained at the inner region of the blank.

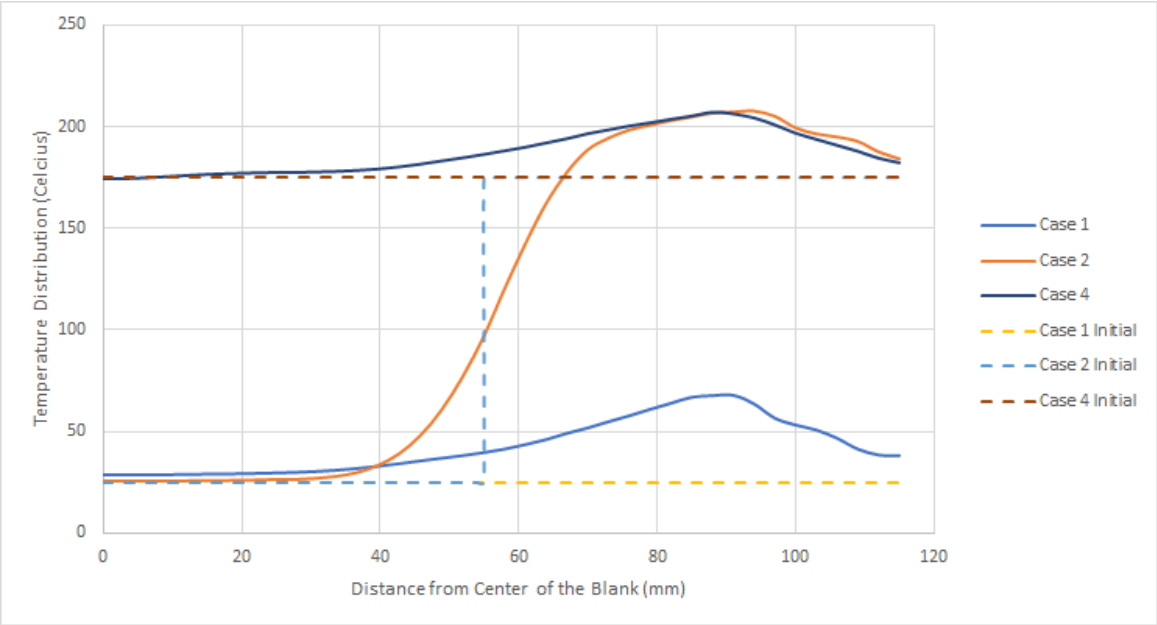

Fig. 10: Temperature distribution vs distance from center of the blank for Cases 1, 2 and 4

Moreover, by increasing the blank holder force to 25000 N, the depth of the cups for failure were determined by using Johnson Cook failure criterion. Having the initial temperature values same in Table 8, height of cup values (punch) are shown when the fracture of the blank initiates. The highest cup height was reached for Case 4. Increasing the temperature of the flange region also helps to reach higher cup height. However, heating the blank at region under the punch results earlier fracture even compared to the room temperature. Initiation of failure of the blank for Case 1 is shown in Figure 12.

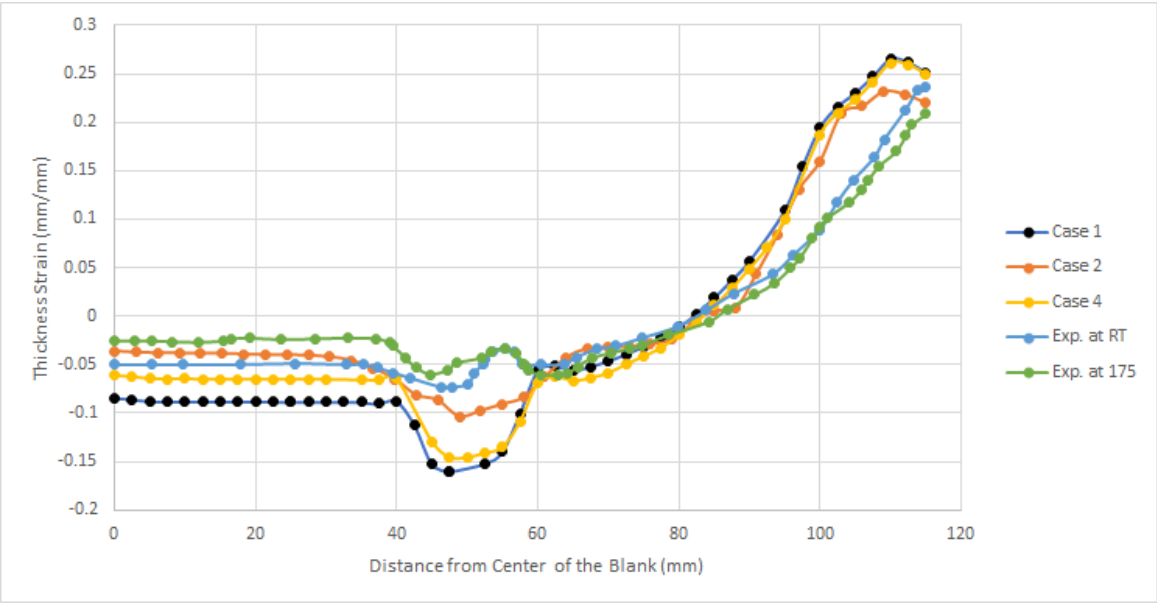

Fig. 11: Thickness strain distribution vs distance from center of the blank for Cases 1, 2 and 4

Table 8: Depth of cup at different local heating cases

	Case 1	Case 2	Case 3	Case 4
Depth of Cup at Beginning of Failure (mm)	54.06	63.87	51.46	69.78

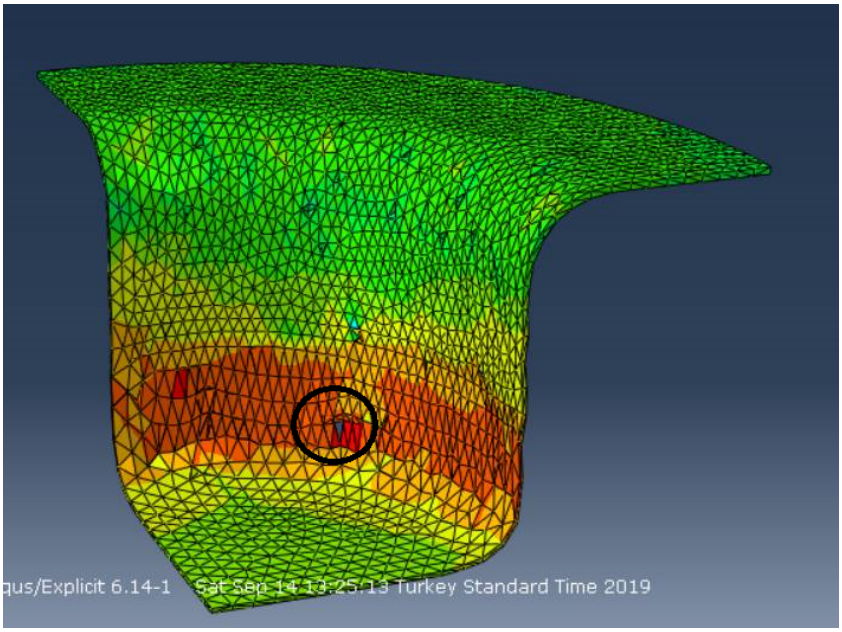

Fig. 12: Beginning of failure for cylindrical deep drawing

HFQ Process and Local Heating of Complex Shaped Blank. HFQ process and local heating of complex shaped blank were simulated for a part. Stages of the forming process are demonstrated in Figure 13. In the first step, the punch forms sheet metal towards the die at the bottom till the sheet touches the die. This first step continues up to contacting the bottom die with sheet metal. In second step the punch at the bottom forms the inner portion of the part whereas the blank holder force is exerted by the springs attached to the fixed to the bottom die. The blank, punch, upper blank holder, bottom punch, bottom die and bottom blank holder were all modeled in ABAQUS.

Mechanical and thermal properties of the blank material AA5754-O and tool steel H13 which are used in all simulations are presented in Table 9. Figure 14 shows the formed part [6].

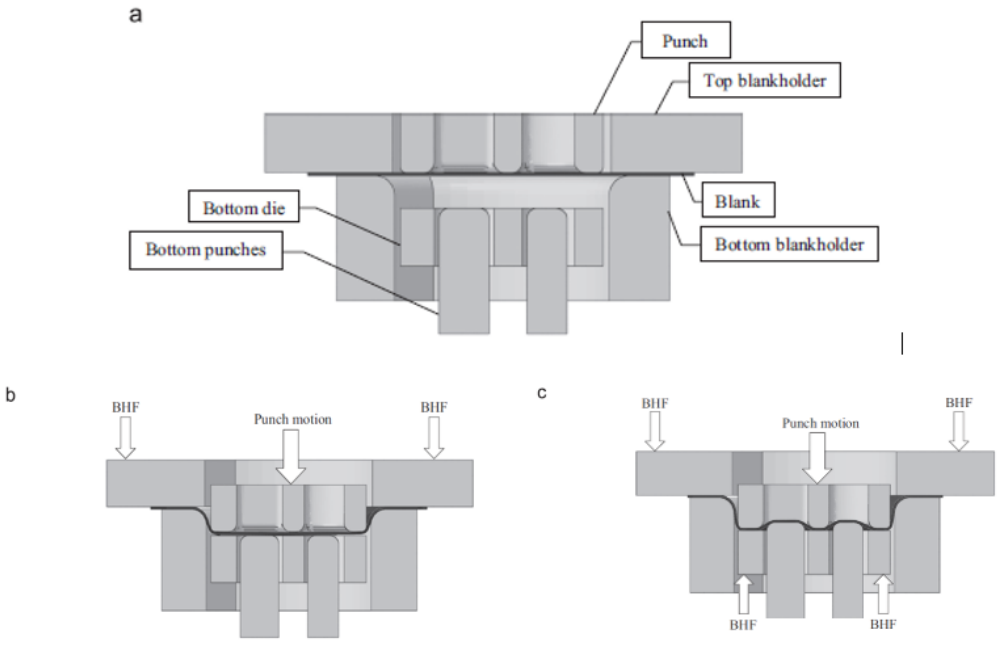

Fig. 13: (a) Initial section of the blank and tools, (b) 1st stage of the process in where BHF is applied top BH, and (c) 2nd stage of the process in where sheet metal contacts with bottom die and BHF is also applied by gas springs. [6]

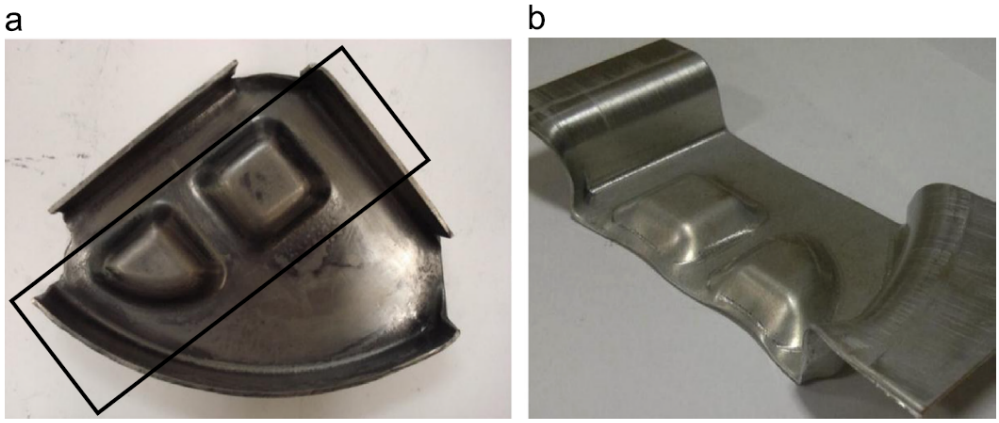

Fig. 14: (a) Formed whole sheet metal shape and trimmed part of the sheet metal and (b) section formed, highlighted by rectangle in (a). [6]

Table 9: Material and thermal properties of blank and tools [6].

	Blank Material	Tool Material
Property	AA5754	H13 Tool Steel
Thermal Conductivity (W/mK)	$147*10^6$	$38*10^6$
Specific Heat (J/mK)	$9.60*10^2$	$4.70*10^2$
Density (kg/m^3)	2700	7800
Poisson's Ratio	0.33	0.3
Young Modulus (MPa)	-	$2.1*10^5$

HFQ processes for the related part were analyzed at 200°C, 350°C and 480°C by using different yield criteria.

In Figure 15, thickness strain distributions of the complex shaped blank obtained by FEM at 200°C are shown. The highest thickness strains are observed at the corner regions of the deformed part. Maximum thinning of the sheet is located at 92 mm along the section. Whereas YLD2003 yield criterion gives the closest results to the experimental results at most of the regions, the results of von Mises yield criterion with kinematic hardening rule deviate significantly from experimental results. At the regions which formed at the second step of the deep drawing process, von Mises with combined hardening rule and Hill48 yield criteria also gave good results.

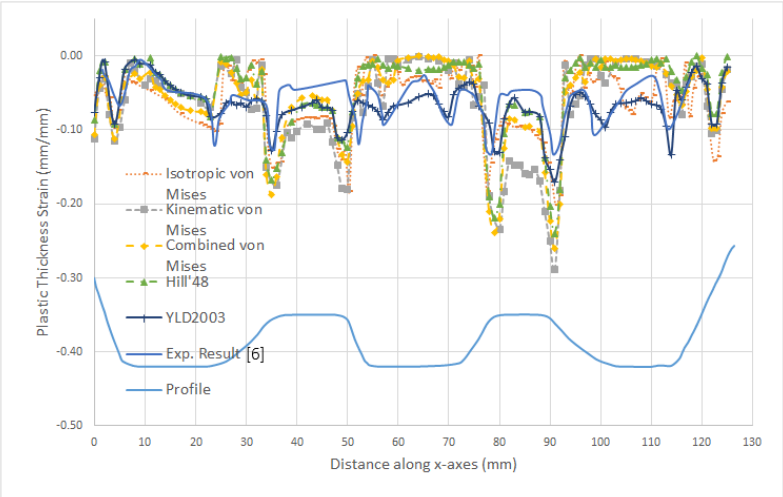

Fig. 15: Plastic thickness strain distributions for different yield criteria at 200°C (HFQ process for complex shape)

In Figure 16, thickness strain distributions of the complex shaped blank obtained by FEM at 350°C are shown. The highest thickness strains are observed again at the corner regions of the deformed part. YLD2003 and Hill48 yield criteria gave the best results that are closer to the experimental results at most of the regions. Kinematic hardening rule with von Mises yield criterion could not predict the thickness strain variation good enough. Other models give closer results to experimental results at 350°C than 200°C.

In Figure 17, simulated thickness strain distributions of the complex shaped blank at 480°C are shown. 480°C is the SHT temperature of AA5754. The highest thickness strains are observed at the corner regions of the deformed part for all models and experiment. YLD2003 yield criterion gave the closest result to the experimental result at most of the regions. von Mises yield criterion with isotropic and kinematic hardening rules predicted the results with a significant difference. Von Mises with combined hardening rule and Hill48 yield criteria gave close results to experimental results at the regions which occur in second step of the deep drawing process.

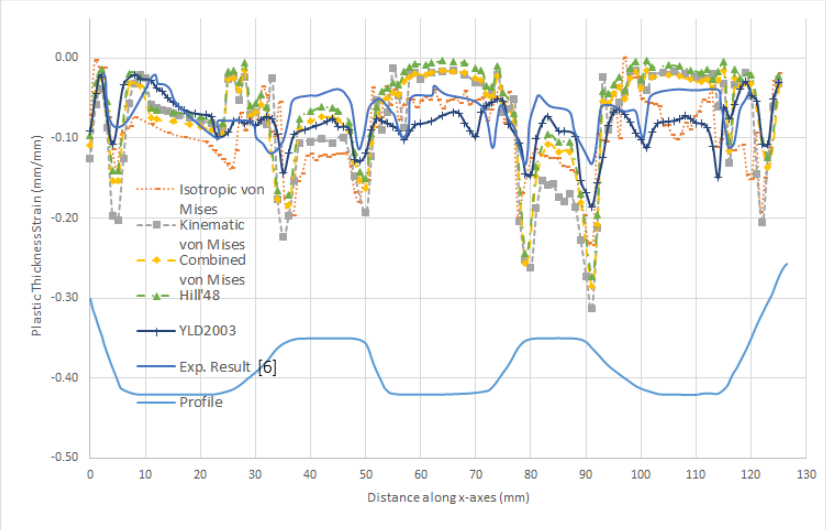

Fig. 16: Plastic thickness strain distributions for different yield criteria at 350°C (HFQ process for complex shape)

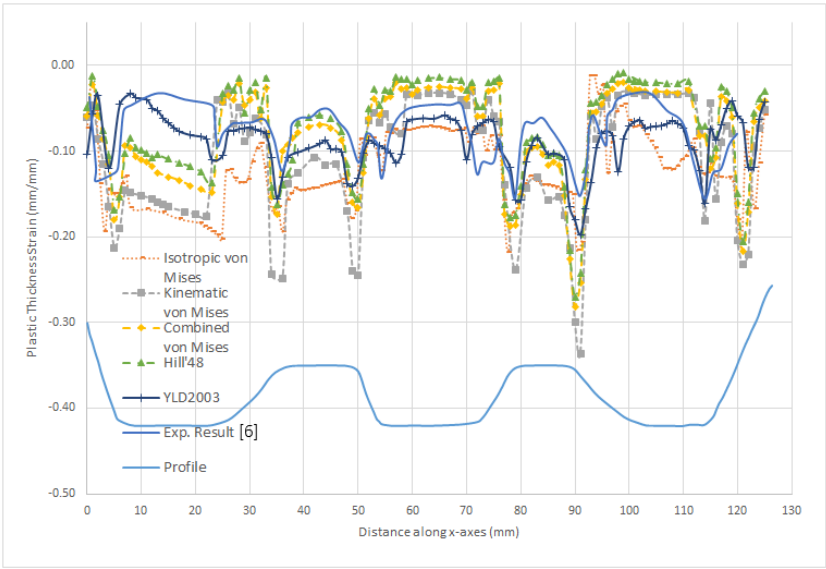

Fig. 17: Plastic thickness strain distributions for different yield criteria at 480°C (HFQ process for complex shape)

For simulating local heating of complex shaped blank, rectangular blank separated into four different parts as shown in Figure 18. Simulations were carried out for five different cases as shown Table 10.

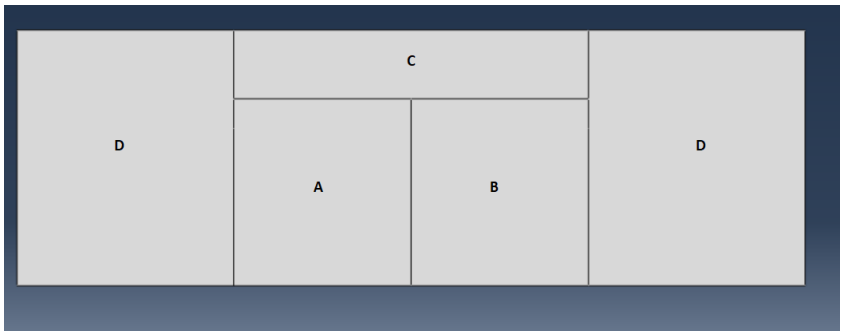

Fig. 18: Partition of rectangular blank.

Table 10: Temperature of the tools and regions of the blank in local heating processes for complex shape

	Case-1	Case-2	Case-3	Case-4	Case-5
Initial Temp. of Region A (°C)	25	200	350	25	350
Initial Temp. of Region B (°C)	25	200	350	25	350
Temperature of Region C (°C)	25	25	25	25	350
Temperature of Region D (°C)	25	25	25	200	350
Temperature of Tools (°C)	20	20	20	20	20

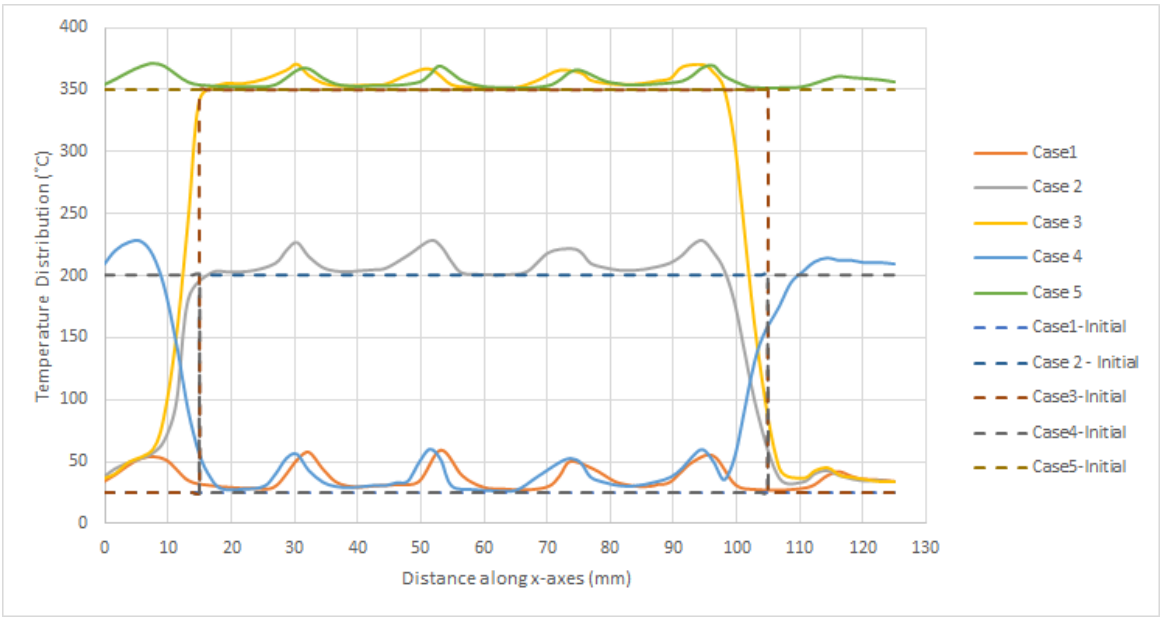

Fig. 19: Temperature distribution with blank distance along x-axis for Cases 1, 2, 3, 4 and 5 (for complex shape)

In Figure 19, temperature distributions of complex shaped blanks are presented for local heating process. Although temperature values of tools and die are 20°C which is lower than temperatures of the blanks for all cases, temperature values of the blanks increased about 25°C during deep drawing process, since a high percentage of plastic work is converted to heat. Higher increases in temperature occur at the corner regions of the blank where maximum thickness strain values are also observed.

According to Figure 20, if the flange region of the blank is heated and temperature of the inner region of the blank is kept at room temperature as in Case 4, more uniform thickness strain distribution is obtained than homogeneous heating of blank as in Case 5. In the deep drawing process of complex shape of AA5754 sheet material, the most uniform shape was obtained with respect to thickness strain at room temperature (Case 1). If the inner region of the blank is heated and the flange region is kept at room temperature, the part has the highest thickness strain values and become thinner as shown in Case 3.

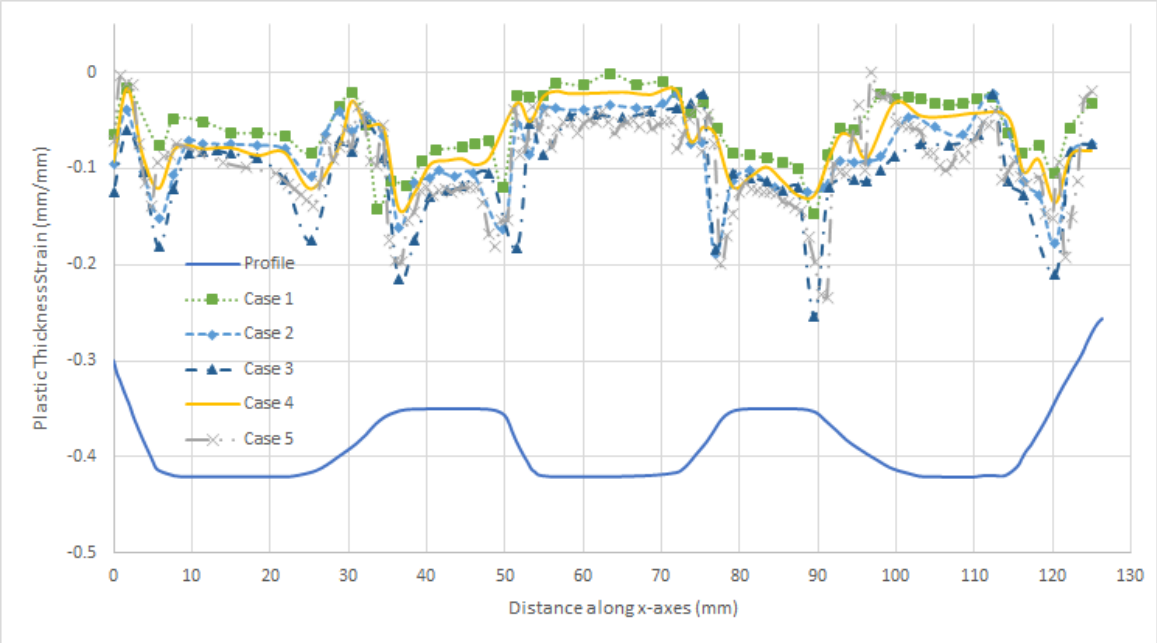

Fig. 20: Thickness strain with distance along x-axis of local heating of complex shape for Cases 1, 2, 3, 4 and 5

Conclusion

In this paper, von Mises yield criteria with isotropic, kinematic and combined hardening rules, Hill48 and YLD2003-8P yield criteria with isotropic hardening and Johnson Cook model are considered for the simulations of deep drawing processes of cylindrical, square and a complex shaped parts at different temperature values by using finite element analysis. Moreover, cylindrical and irregular complex shaped blanks were analyzed with local heating. By using Johnson Cook failure criterion the maximum cup height values were determined for cylindrical deep drawing process. HFQ process was also investigated with different temperatures including SHT for complex shaped blank. The following items were concluded from this paper:

- Thickness strains of AA5754 sheet materials decrease with increasing temperature for cylindrical deep drawing process at most of the regions of the blank.
- While thickness strains of AA5754 sheet material increase with increasing temperature at region under the punch for square deep drawing, they decrease with increasing temperature at cup wall and flange regions.

- For HFQ process, thickness strain of the complex shaped part increased and thickness homogeneity of this part decreased with increasing temperature.
- It is observed that as temperature increases for relatively simple forming processes such as cylindrical, thickness change decreases under both punch and flange region whereas at room temperature thickness change is greater for both regions. On the other side as the part shape becomes complicated tensile thickness strains decrease whereas compressive thickness strains increase.
- YLD2003 yield criterion gives more reliable results with respect to the thickness strain, if compared with the other used yield criteria.
- For local heating process of circular blank, heating the flange region of the blank and keeping the inner temperature at room temperature gave more uniform results and thickness strain decreases compared to homogeneous heating of the blank.

References

[1] M. A. Basril, H. M. Teng, M. Azuddin, and I. A. Choudhury, "The effect of heating temperature and methods towards the formability of deep drawn square metal cup," *IOP Conference Series: Materials Science and Engineering,* vol. 210, no. 1, 2017.

[2] H. Laurent, J. Coër, P. Y. Manach, M. C. Oliveira, and L. F. Menezes, "Experimental and numerical studies on the warm deep drawing of an Al-Mg alloy," *International Journal of Mechanical Sciences,* vol. 93, pp. 59–72, 2015.

[3] N. Abedrabbo, F. Pourboghrat, and J. Carsley, "Forming of AA5182-O and AA5754-O at elevated temperatures using coupled thermo-mechanical finite element models," *International Journal of Plasticity,* vol. 23, no. 5, pp. 841–875, 2007.

[4] F. Barlat, J. Brem, J. Yoon, K. Chung, R. Dick, D. Lege, F. Pourboghrat, S. H. Choi, and E. Chu, "Plane stress yield function for aluminum alloy sheets part 1 : theory," *International Journal of Plasticity,* vol. 19, pp. 1297–1319, 2003.

[5] R. H. Demirkol, Analysis of Effects of Temperature Variation on Deep Drawing Process Using Different Constitutive Laws, MSc. Thesis, Middle East Technical University, 2019.

[6] O. El Fakir, L. Wang, D. Balint, J. P. Dear, J. Lin, and T. A. Dean,"Numerical study of the solution heat treatment, forming, and in-die quenching (hfq) process on aa5754," *International Journal of Machine Tools and Manufacture,* vol. 87, pp. 39–48, 2014.

[7] F. Cogun and H. Darendeliler, "Comparison of different yield criteria in various deep drawn cups," *International Journal of Material Forming,* vol. 10, no. 1, pp. 85–98, 2017.

[8] R. Hill, A Theory of the Yielding and Plastic Flow of Anisotropic Metals , Proc. R. Soc. London 193, 281-297 vol. 10, no. 1, pp. 85–98, 2017.

[9] H. K. Farahani, "Determination of Johnson Cook Plasticity Model Parameters for Inconel718," no. October, 2017.

[10] H. Aretz, A non-quadratic plane stress yield function for orthotropic sheet metal , J Mat Proc Technol, 168:1–9, 2005.

[11] J. Winklhofer, G. Trattnig, C. Lind, C. Sommitsch, and H. Feuerhuber, "Simulation of aluminium sheet metal deep drawing at elevated temperatures using LS-Dyna," *AIP Conference Proceedings,* vol. 1252, pp. 927–934, 2010.

[12] M. Rodriguez-Millan, D. Garcia-Gonzalez, A. Rusinek, and A. Arias, "Influence of Stress State on the Mechanical Impact and Deformation Behaviors of Aluminum Alloys," *Metals,* vol. 8, no. 7, p. 520, 2018.

[13] A. H. van Deen Boogaard, Thermally Enhanced Forming of Aluminium Sheet, Ph.D. Thesis, University of Twente, 2002.